Karlsruher Institut für Technologie

FAKULTÄT FÜR PHYSIK

PHYSIKALISCHES PRAKTIKUM FÜR FORTGESCHRITTENE

PRAKTIKUM MODERNE PHYSIK

Gruppe Nr. _____ Kurs: **Mo1** **Mo2** **Mi3**

zutreffendes bitte ankreuzen

aktuelles Semester angeben

Versuch: _____

Namen: _____

_____

Assistent: _____

durchgeführt am: _____

Protokollabgabe am: _____

_____

vom Betreuer auszufüllen

Note gesamt [+] [0] [-]

Anerkannt: _____

(Datum Unterschrift)

Datum Rückgabe: _____

Bemerkung:

Contents

List of Figures

1. Introduction

Silicon strip detectors have become a cornerstone in high-energy physics, serving as an indispensable tool in the detection and analysis of charged particles. Utilized extensively in experiments such as those conducted at the Compact Muon Solenoid (CMS) at the Large Hadron Collider (LHC), these detectors provide high-resolution tracking of particle trajectories. The operational principle of silicon strip detectors is predicated on the semiconductor properties of silicon, which, when interacting with an ionizing particle, facilitate the creation of electron-hole pairs. The process of pair creation and subsequent current generation is exquisitely sensitive to the energy and path of the passing particles, making these detectors highly effective for particle tracking.

The principle of operation of a silicon strip detector can be explained by the interaction of ionizing particles with the silicon substrate, as governed by the Bethe formula. The energy deposition from these interactions results in the excitation of silicon atoms and the subsequent creation of electron-hole pairs, provided the energy exceeds the threshold of 3.6 electronvolts.

A key feature of the silicon strip detector is the ability to discern the trajectory of the incident particle. This is achieved through the implementation of p-n junctions within the silicon lattice as shown in Figure 1.2, forming a depletion zone. When a particle passes through this zone, the electrical field present prompts the separation of the electron-hole pairs, generating a current measurable by the readout electronics. The application of a reverse bias voltage across the p-n junctions further enhances this effect by widening the depletion zone, thereby improving the detector's resolution and sensitivity.

In addition to particle tracking, when subjected to a magnetic field, these detectors can also provide information on the momentum and charge parity of the particles. This is due to the Lorentz force acted upon by the magnetic field, which causes a deflection in their trajectory, allowing the determination of these properties based on the curvature of the path taken through the detector.

To further enhance the spatial resolution, silicon strip detectors are configured in arrays, with multiple p-n junctions placed in lines next to each other. This arrangement allows for a detailed reconstruction of the particle trajectories, making it possible to perform precise vertexing and momentum measurements. Such granularity is crucial for experiments where the understanding of particle interactions and decay mechanisms are of paramount interest.

The implementation of silicon strip detectors in high-energy physics experiments requires careful consideration of factors such as radiation hardness, signal-to-noise ratio, and the overall integration with other detector systems. With the advancements in microfabrication techniques, the design and manufacturing of silicon strip detectors have become increasingly sophisticated, enabling their deployment in increasingly challenging experimental environments.

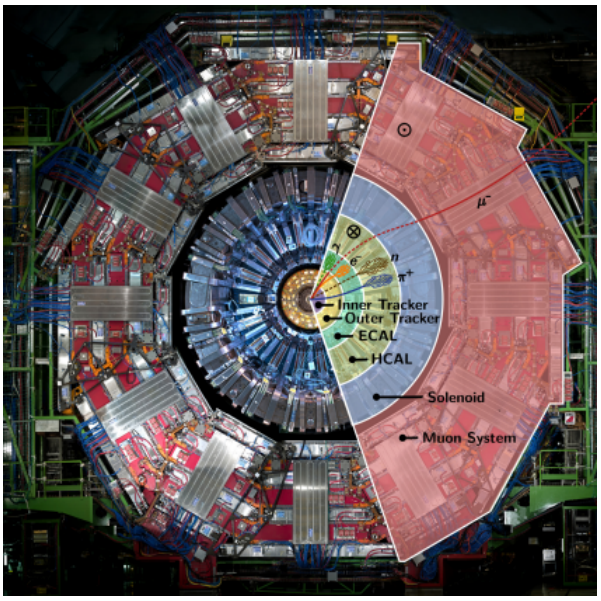

Figure 1.1: A cross-section through the CMS detector shows the different subsystems including the particles that can be detected in each case.

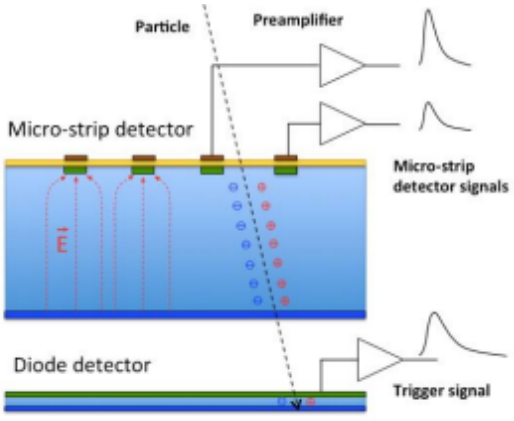

Figure 1.2: Sketch of signal formation and the EASY diode trigger

This report proceeds to describe the application of silicon strip detectors in a practical experimental context, detailing the methods of data acquisition and subsequent analysis. Through this exploration, the report aims to elucidate the intricate balance between theory and practice in the domain of particle detection.

Experimental Motivation

The experiment detailed herein is designed to investigate the properties of silicon strip detectors under controlled conditions. The objectives are to demonstrate the functionality of these detectors in a laboratory setting and to analyze the data obtained from a series of measurements. The insights gained from this experiment are intended to contribute to the broader understanding of detector performance, particularly in the aspects of energy resolution, efficiency, and the impact of radiation damage over time.

2. Experimental Setup

This chapter delves into the practical aspect of the study, providing a detailed description of the experimental setup and the procedures followed for data acquisition. The objective is to offer a comprehensive understanding of the methodology employed to exploit the capabilities of silicon strip detectors in a controlled environment. It is structured into two primary sections: the Experimental Setup, which outlines the configuration of the instruments and equipment utilized. Data Acquisition, which describes the capabilities of the software that is used and the details of each mode that is necessary for different steps and runs. The next chapter, Experimental procedure & Data Analysis will describe the systematic approach taken to capture and record the data and subsequently, their analysis and interpretation. The intricacies of the setup are pivotal in ensuring the accuracy and reliability of the measurements, which, in turn, are crucial for the accurate interpretation and understanding of the experimental results. The interplay between the precision of the setup and the granularity of data collection forms the backbone of this research, reflecting the meticulous nature of scientific inquiry. This chapter not only documents the methodological steps taken but also sets a precedent for reproducibility, a core tenet of experimental science. The subsequent sections will describe the considerations and protocols in place that ensure the fidelity of the data acquisition process

2.1 Experimental Setup

The experimental setup for investigating the properties of Silicon Strip Detectors (Si-Strip Detectors) involves a comprehensive array of equipment and methodologies designed to characterize the sensor's electrical properties and characteristics, such as pitch size. This section delineates the setup and preparation for these experiments.

The EASY (Educational Alibava System)

The core of the experimental setup is the Educational Alibava System (EASY), a state-of-the-art system designed for the investigation of Si-Strip Detectors. The EASY comprises two primary components: a control unit and a sensor unit. These units, shown in Figure 2.1 are interconnected through a flatband cable, facilitating data transfer. Additionally, an optical fiber and a brown LEMO cable are employed for triggering and data readout processes.

- **Control Unit:** This unit serves as the central hub for controlling the experiment, setting bias voltages, and reading out data. It includes various ports and knobs for adjusting settings and connecting to the sensor unit and a PC for data acquisition.
- **Sensor Unit:** The sensor unit incorporates an electronic board with the BEETLE readout ASIC, which provides 128 analog input channels. This unit is responsible for processing signals from the Si-Strip sensor.

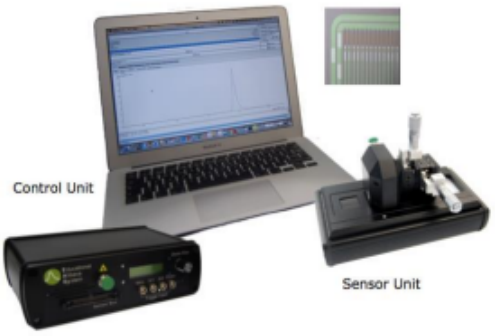

Figure 2.1: EASY system with the Control Unit, the Sensor Unit and the acquisition program Alibava-gui running in the computer.[2]

Sensor Stage and Readout

The sensor stage, an essential component of the experimental setup, is meticulously engineered to hold the Si-Strip sensor. It includes provisions for precise sensor positioning and facilitating connections to the readout system. A critical enhancement in the setup is the inclusion of a diode trigger placed below the sensor, instrumental in initiating the readout process. This trigger mechanism ensures the readout is precisely synchronized with the sensor's detection events.

The sensor unit, shown in Figure 2.2, is versatile, offering two modes of operation, as illustrated in Figure 2.3, a radioactive source mode and a laser source mode. This dual-mode functionality allows for comprehensive investigation under different conditions, enhancing the experiment's scope. In both modes, the readout is executed by the BEETLE ASIC, which operates at a clocked analog pipeline frequency of 40 MHz. The system's design permits adjustments in latency to counter system delays, thus ensuring accurate timing for signal readout. Such a configuration is crucial for the precise capture and interpretation of data from the Si-Strip sensor.

Sensor Specifications

The Si-Strip sensor used in the experiment, shown in Figure 2.4, is characterized by a specific pitch and active width, essential for understanding its response to particle interactions. The sensor's architecture, namely the p-in-n design, is critical for its functionality in detecting charged particles.

Experimental Procedures

The experimental procedures involve various steps to fully characterize the Si-Strip sensor:

1. **Bias Voltage Setting:** The bias voltage is adjusted using the control unit to optimize the sensor's operating conditions.
2. **Triggering and Data Readout:** The triggering mechanism is set up using the optical fiber and LEMO cable, with specific latency settings to synchronize the readout process.
3. **Data Acquisition:** Data is acquired through the control unit and transferred to a PC for analysis. This process involves capturing the sensor's response to particle interactions and other stimuli.

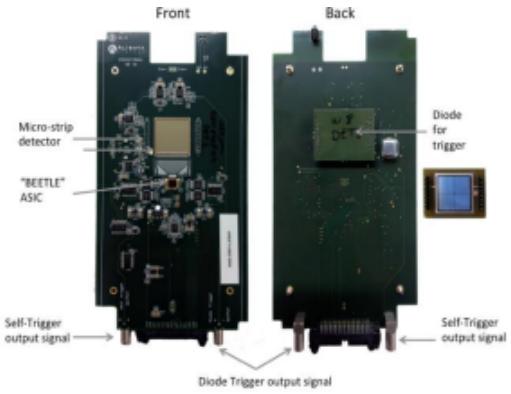

Figure 2.2: Sensor Unit holding the micro-strip detector and the BEETLE in the front side and the Diode for trigger proposes in the back. The Board have two connectors for the trigger signal: Diode Trigger and Self-Trigger.[2]

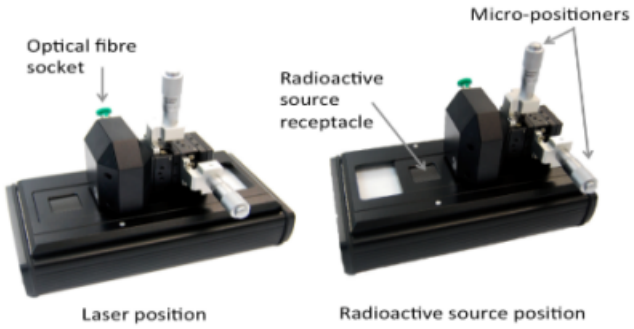

Figure 2.3: Sensor stage positions

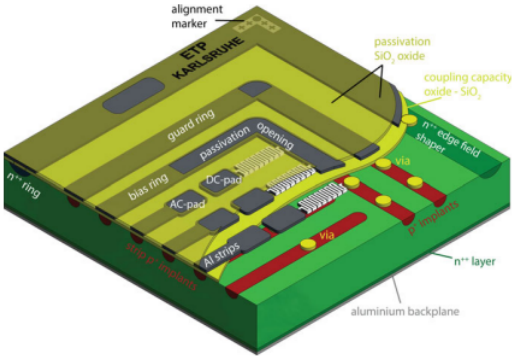

Figure 2.4: A p-in-n strip sensor

Leakage Current and Temperature Control

An essential aspect of the experimental setup is monitoring the leakage current and temperature of the Si-Strip sensor. The control unit is equipped to measure these parameters, providing insights into the sensor's operational stability and efficiency.

Software for Data Analysis

The data acquired from the EASY is analyzed using specialized software, which interprets the sensor's response, processes the signals, and extracts relevant information for characterizing the Si-Strip sensor's properties.

2.2 Data Acquisition

Software Utilization for Data Acquisition

Data acquisition in the investigation of Silicon Strip Detectors was executed using a comprehensive software suite designed to control the experimental setup, manipulate the parameters, and capture the resultant data. The software, integral to the experimental procedure, enabled precise data manipulation and effective data collection.

Pedestal Run

Initially, a pedestal run was conducted to establish the baseline noise level for each channel. This baseline noise, or 'pedestal noise', originates from the electronic components in the detection system and is present even when the detector is not actively measuring any particles or radiation. It is an intrinsic part of the system's operation.The pedestal value for a channel is calculated as the mean of the ADC counts when no signal is present, adjusted for common mode noise which is a collective fluctuation affecting all channels similarly, often due to environmental factors like electromagnetic fields:

$$P(i) = \frac{1}{N} \sum_{k=1}^{N} ADC(i,k) - D(k) \tag{2.1}$$

Where $P(i)$ is the pedestal value for channel i, N is the number of readings, $ADC(i,k)$ is the ADC count for channel i at reading k, and $D(k)$ represents the common mode noise at reading k.

Noise Characterization

The software's functionality extended to the characterization of noise, which is a combination of the pedestal and additional fluctuations. The total noise for a channel is defined as:

$$N(i) = \sqrt{\frac{1}{N-1} \sum_{k=1}^{N} (P_c(i) - \bar{P}_c(i))^2}, \tag{2.2}$$

Signal Acquisition

For signal acquisition, the software facilitated the capture of ADC counts across the channels when the detector was exposed to stimuli (e.g., particle interaction). The signal for each channel is the ADC count minus the pedestal, adjusted for common mode:

$$S(i,k) = ADC(i,k) - P(i,k) - D(k) \tag{2.3}$$

Latency Adjustment

The software provided the capability to adjust the latency, which refers to the delay between the actual physical interaction —like a particle passing through a detector— and the electronic signal formation that is subsequently processed. This delay is important for ensuring that the data acquisition system is precisely synchronized with the event it's meant to record. The latency was tuned to ensure the capture of signals at the moment they reach their maximum strength.

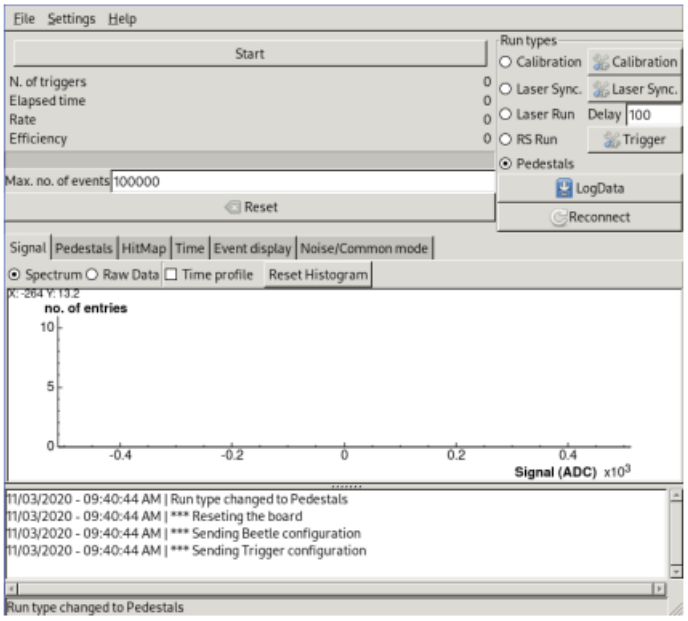

Figure 2.5: The alibava-gui interface.

Calibration

Calibration runs were essential for converting ADC counts into meaningful physical quantities. The calibration process involved injecting known charges and recording the corresponding ADC counts. A conversion factor was then derived from these data.

Data Analysis

Finally, the software suite included tools for data analysis. This involved processing the captured ADC counts, subtracting the pedestal, applying the calibration factors, and extracting meaningful physical measurements from the experiment.

Clustering

The clustering algorithm in Alibava analysis identifies clusters of channels with signals above a certain threshold. This process involves defining seeds and neighbors within the cluster and discarding channels that do not meet these criteria.

In summary, the software used in the experiment was pivotal in conducting the pedestal run, characterizing noise, adjusting latency, and calibrating the system, all of which were crucial for accurate data acquisition and analysis.

3. Experimental Procedure & Data Analysis

3.1 Pitch Measurement

The aim of this exercise was to ascertain the pitch of the detector utilizing the built-in laser system.

1. **Setting the Bias Voltage:** The bias voltage was initially set at 110 V to optimize the detector's sensitivity to the laser stimulation.
2. **Laser Synchronization and Delay Adjustment:** The laser was then synchronized with the system's timing, and the delay was fine-tuned to capture the peak sensor response.
3. **Execution of Laser Runs:** A series of laser runs were executed, focusing the laser onto the detector's surface.
4. **Laser Positioning:** In increments of 10 µm, the laser was shifted perpendicular to the strip direction over a span of at least 320 µm to accurately measure the detector's pitch.
5. **Data Collection and Analysis:** The collected data, representing the signal as a function of laser position, was analyzed to determine the pitch of the detector. This information is crucial as it defines the spatial resolution and the minimum distance at which two points can be distinctly identified by the sensor.

The results of this exercise are depicted in Figure 3.1. The plot illustrates the charge distribution as a function of the laser position. Unlike peaks indicating alignment with the strips, the minima in the signals for strips 67, 68, and 69 are important for the analysis. These minima correspond to the laser scanning across the gaps between the strips, which are coated with a reflective material. The distance between these minima represents the pitch of the detector, which is the distance between the centers of adjacent strips.

The detector pitch, calculated as the distance between the minimums of the charge distribution, is found to be $d = 160 \pm 5\mu m$, which is consistent with the expected value. The precision of the measurement is evidenced by the consistent spacing between signal minimums. This outcome validates the accuracy of the pitch measurement procedure and the detector's design specifications.

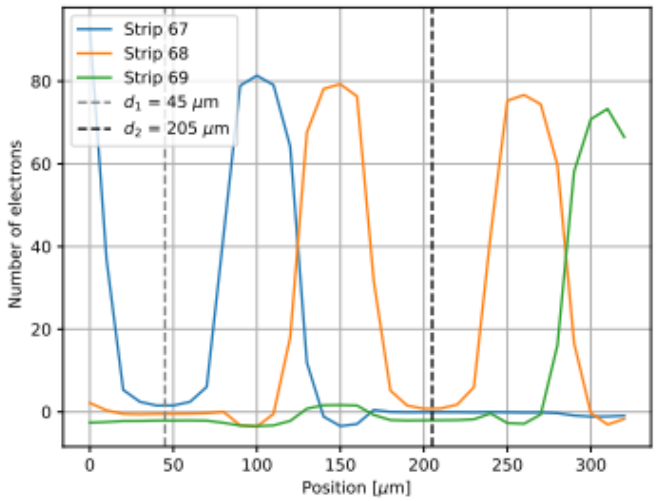

Figure 3.1: Signal deposition by the laser bean in three consecutive strips obtained by moving the laser in 10μm steps perpendicular to the strips. The signal recorded by strip 67 is represented in blue, in orange the signal in strip 68 and in green the signal in strips 69.

3.2 Electrical Characterization

The electrical characterization of the Silicon Strip Sensor was conducted to assess the sensor's performance and identify its electrical properties.

Importance of IV Characteristics

The IV curve is critical for determining the sensor's noise at various voltage levels. By ramping the voltage from 0 V to 110 V in 10 V increments and recording the bias current at each step, one can assess the presence of any material defects or breakdowns.

Purpose of CV Curve

Meanwhile, the CV curve is essential for evaluating the sensor's capacitance as a function of the applied bias voltage. This measurement is indicative of the depletion region's width and the doping concentration within the sensor. The CV curve is utilized to ascertain the full depletion voltage and to monitor the changes in capacitance, which are directly related to the active volume of the detector.

Voltage Ramp and Bias Current Recording

In practice, a voltage ramp from 0 V to 110 V is executed, increasing in steps of 10 V, to observe the sensor's behavior under different electric fields. At each voltage step, the corresponding bias current was recorded. This procedure enables to construct the IV curve, which is pivotal for understanding the leakage current of the detector under varying electric potentials.

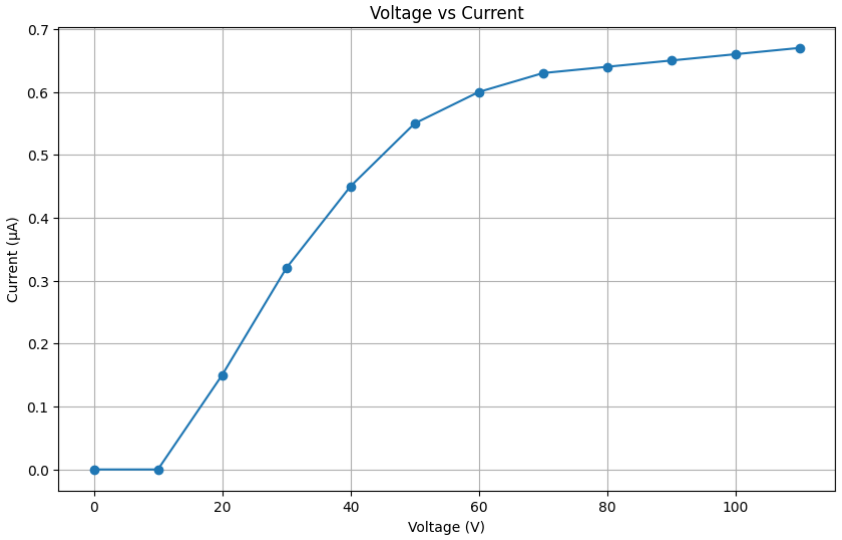

Figure 3.2: Plot of the IV characteristic of the Si-detector.

Anticipated Changes Post-Irradiation

If the sensor is exposed to radiation, defects can form in its silicon structure. These defects often lead to an unwanted increase in electrical leakage, noticeable even at lower voltages. The resulting IV curve would differ from that of an undamaged sensor, showing a sharper increase, which is indicative of the additional charge carriers generated by radiation damage in the sensor's depleted region.

IV Curve Analysis

The resulting IV curve, shown in Figure 3.2, reveals the sensor's behavior as the voltage increases. This IV curve is critical for several reasons: Firstly, it typically allows one to observe the point at which the breakdown effects may occur. Due to the nature of the sensor's construction, where edges are cut by machinery, there can be defects at the boundaries. To mitigate potential issues arising from these imperfect edges, a guard ring is employed. This guard ring helps in achieving well-defined edges for the sensor, which is crucial for uniform electric fields and preventing edge breakdown effects. As a result of this implementation, one may not observe a sharp saturation current level. Instead, the current increases gradually, reflecting the progressive extension of the depletion zone towards the sensor's edges. Secondly, the curve aids in understanding the effects of thermal excitation on the charge carriers. With increasing voltage, charge carriers are energized, and their thermal excitation contributes to the current. This contribution continues until it appears to stabilize, but due to the aforementioned edge treatments, the stabilization may not be as pronounced as in ideal conditions. Thus, the expected plateau may instead be a region where the current increment slows but does not reach a perfectly constant level.

The recorded data shows a gradual increase in current with increasing voltage, which is expected due to the enhanced collection of thermally generated charge carriers. However, the current does not continue to rise indefinitely; it begins to plateau, suggesting that the depletion region has reached its maximum extent and the bulk of the sensor, that is defined by the spatial extensions of the guard ring, is fully depleted. This behavior is consistent with the expected characteristics of a well-functioning silicon strip sensor. The data indicates that as voltage increases, the current also rises due to more charge carriers being collected and follows a square root relation to the bias voltage.

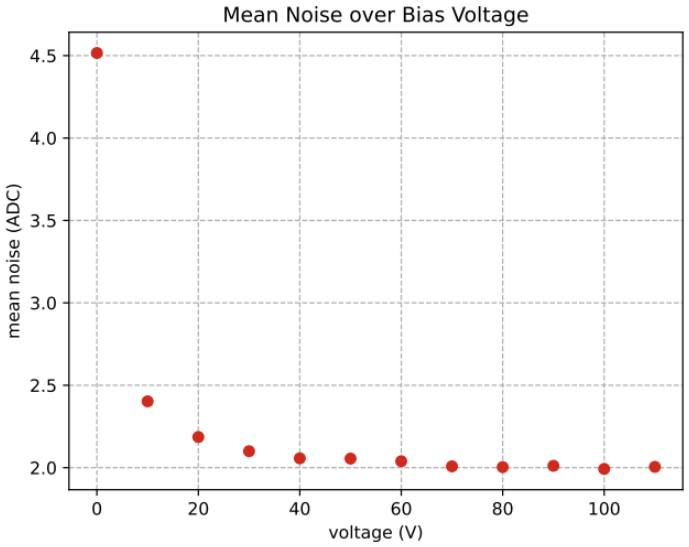

Figure 3.3: Mean noise for different bias voltages.

3.3 Noise Characterization

In every measurement process, understanding and mitigating noise is crucial to ensure the accuracy of the data collected. For the Silicon Strip Sensor, various sources of noise can influence the readings, and identifying these is essential for reliable operation.

Bias Voltage Influence on Noise

The sensor bias voltage is an important parameter in the operation of the detector and can significantly impact the noise levels. An increase in bias voltage typically leads to a reduction in capacitance, specifically the junction capacitance associated with the depletion region of the sensor, which decreases the noise because noise is inversely proportional to capacitance. Additionally, this results in an increase in depletion width, affecting the noise characteristics.

Bias Voltage Ramp and Noise Measurement

For this exercise, the bias voltage was systematically increased from 0 V to 110 V in increments of 10 V. At each step, a pedestal run with $n_{trig} = 5000$ was saved. These runs allow for a detailed analysis of the noise levels at varying bias voltages.

The result of this exercise is depicted in Figure 3.3, which shows the mean noise as a function of the bias voltage. A notable observation from the plot is the initial decrease in noise levels as the bias voltage increases from 0 V, reaching a plateau after a certain voltage value. This behavior is consistent with the reduction in capacitance as the sensor approaches full depletion, leading to a decrease in electronic noise. This causes noise to decrease, even though the leakage current is increasing with the increasing voltage. Once full depletion is reached, the noise levels stabilize as the bias voltage continues to increase, indicating that the sensor operates within its optimal range. The plateau in noise levels suggests that the sensor's electronic components are not introducing additional noise, and the system is stable across the range of operational voltages.

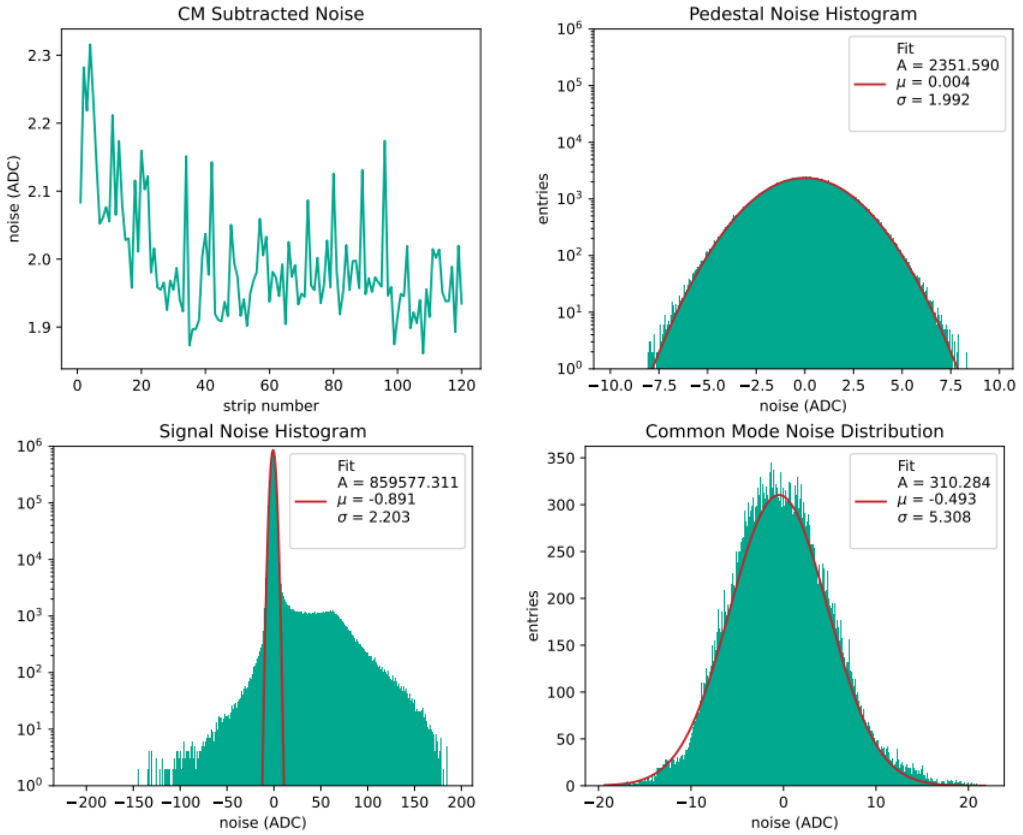

Figure 3.4: In the top left, the noise per strip histogram, where the common mode noise is already subtracted can be seen. The histogram in top right is showing the result of the pedestal runs. Signal noise histogram, depicted in the bottom left is to find the peak of the noise value to subtract for further analysis. The histogram in the bottom right is showing the distribution of the common mode noise.

Understanding Pedestal Noise

The pedestal is a measure of the baseline signal that a sensor outputs in the absence of any true signal. It is crucial to determine this baseline to correct the actual signal measurements. A pedestal run is performed to measure this baseline noise level for each channel of the detector. During such a run, the readout system is triggered without the presence of a signal, and the mean output is recorded and fitted with the available algorithm. This mean value, known as the pedestal, is then subtracted from subsequent measurements to obtain the true signal.

Common Mode Noise and Its Mitigation

Common mode noise is a systematic noise that affects all channels of the detector uniformly. It can arise from fluctuations in the power supply, environmental interferences, or electronic components within the readout system. To eliminate common mode noise, a common practice is to calculate the average signal across all channels for each event and then subtract this value from the individual channel measurements, thus removing the noise component that is common to all. The figure Figure 3.4 is illustrating the analysis of the data to obtain the pedestal noise, common mode noise and it's distribution and the noise per strip where the common mode noise is already subtracted.

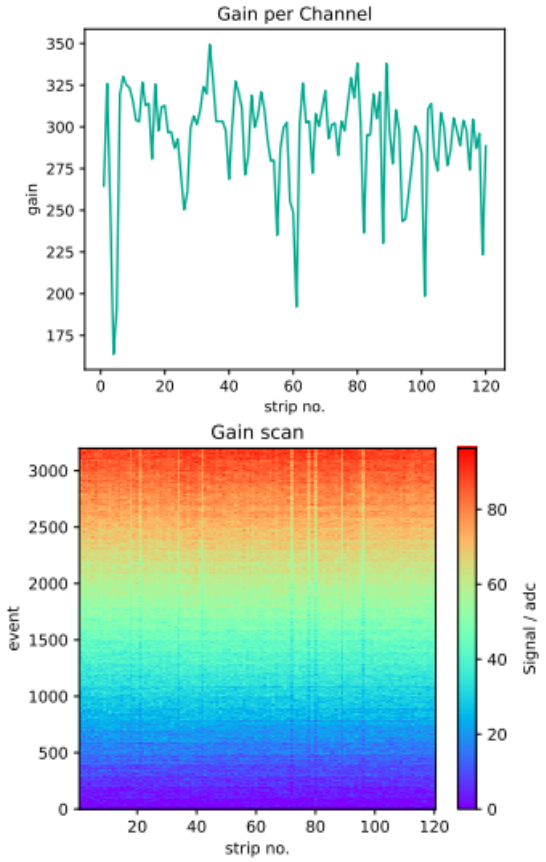

Figure 3.5: Gain per channel on top, indicating the conversion factor between the known charges and the ADC counts. Gain scan on bottom is implying a linear conversion between ADC and electron counts.

Quantifying Noise

The RMS (Root Mean Square) value of noise is computed to provide a statistical measure of the noise's variation. It is calculated by taking the square root of the average of the squared deviations of the corrected pedestals from the mean value. This RMS noise calculation is performed after pedestal and common mode noise subtraction, giving a more accurate depiction of the inherent noise within the system.

3.4 Calibration

Calibration is a critical process in the experimental setup to ensure that charge collection signal measurements are accurate and reliable.

Purpose of Calibration

Calibration is necessary to translate the raw data from the detector into meaningful physical quantities. It establishes a relationship between the known input signals (in terms of charge) and the system's response (in terms of ADC counts). This step is crucial for subsequent measurements to accurately reflect the charge collected by the sensor.

Calibration Procedure and Sources of Error

To perform a calibration run, the system is set to a stable operating bias voltage—110 V in this case—to ensure consistent conditions during the measurement. Known charge pulses are then injected into the system, and the corresponding ADC counts are recorded. The

relationship between the injected charge and the ADC counts forms the calibration curve, which is used to derive the conversion factor for actual experimental data. The conversion factor can be read as $\tilde{3}00$ from the gain per channel plot, shown in Figure 3.5. Despite the fact that gain per channel is varying across the strips, a general statement can be made about it's trend.

Sources of error in calibration can include fluctuations in temperature, electronic noise, variations in the injected charge, and instability in the bias voltage. These factors can introduce uncertainties in the calibration curve, affecting the precision of the conversion factor.

Determining Gain from Calibration Curves

The script `alibava-analysis/analysis/gain.py` is utilized to analyze the calibration runs and extract the gain from the calibration curves. The gain is derived by fitting a function to the calibration data points, which represents the sensor's response to varying charge levels. This fitting process allows for the determination of the gain factor, which is essential for converting the ADC counts into an actual charge measurement. The accuracy of this factor is paramount, as it directly influences the precision of subsequent charge collection measurements.

3.5 Clustering Algorithm

When a charged particle passes through the sensor, it generates charge that is collected by multiple strips, forming what is known as a cluster. The clustering algorithm is designed to identify these clusters and ascertain their properties, which can provide insights into the trajectory and angle of the incoming particles.

- **Cluster Identification:** A cluster is identified as a collection of neighboring channels that register a signal. This signal is due to the charge dispersed by a traversing particle.
- **Seed and Neighbor Definition:** Within a cluster, certain strips register higher signals than others. These are designated as seeds and are defined by a signal that surpasses a predefined threshold, known as the seed cut. Neighboring strips with signals above a different, usually lower, threshold—known as the neighbor cut—are also included in the cluster.
- **Seed Cut and Neighbor Cut:** The seed cut is typically set higher to identify the most probable path of the particle through the sensor, while the neighbor cut is lower to include adjacent strips that have collected some charge as the particle's ionization path is spread out due to diffusion and other effects.
- **Cluster Size Interpretation:** The size of the cluster, which is the number of strips included, can be indicative of the particle's angle of incidence. Large clusters can imply that the particle is entering the strip with a shallow angle, causing it to disperse its charge over a greater number of strips. Conversely, cluster sizes of one or two are generally expected for particles that strike the sensor perpendicularly. This behavior can also be seen from the full-run data. The Figure 3.6 is indicating that, most of the particles are entering the sensor perpendicularly in the full-run, that will be explained and analysed in the following section.
- **Discarding Non-Seeds and Non-Neighbors:** Strips that do not qualify as either seeds or neighbors are excluded from the cluster , as they are unlikely to have collected significant charge from the particle interaction. This exclusion helps to minimize the inclusion of noise and ensures that the cluster size is a true representation of the particle's path through the sensor.

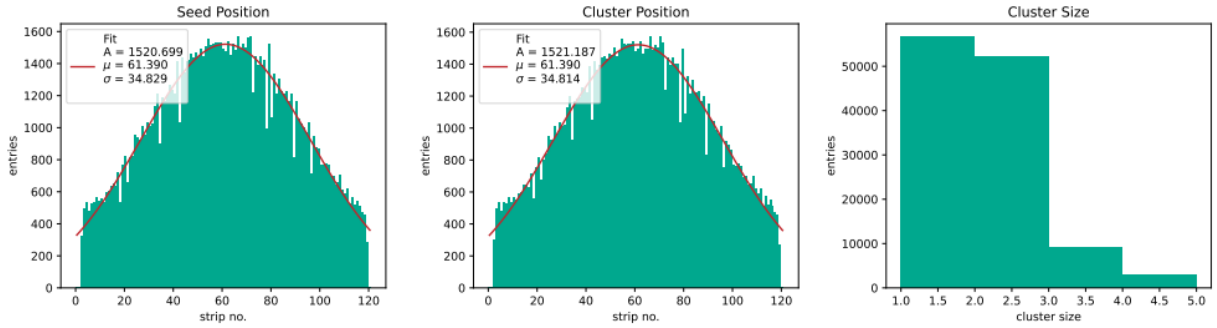

Figure 3.6: The histogram on the left is showing the strips that received a signal, that is above seed cut threshold. The histogram in the middle is depicting the cluster positions and number of entries across the strips. The histogram on the right is indicating the cluster size, which implies the entry-angle of the particles into the sensor.

The efficiency and accuracy of the clustering algorithm are crucial for the precise reconstruction of particle trajectories and for the determination of the sensor's performance characteristics. Proper calibration of the seed and neighbor thresholds is essential for the algorithm to distinguish between actual particle-induced signals and background noise, ensuring reliable data for subsequent analysis.

3.6 Full Run Analysis

Introduction to Full Run Analysis

The comprehensive analysis of the Silicon Strip Detectors, aims to elucidate the detectors' sensitivity and response to particle interactions, with a particular focus on minimum ionizing particles (MIPs). The choice of Strontium-90 (Sr-90) as the radioactive source is strategic, given its beta decay to Yttrium-90, which in turn mimics the behavior of MIPs. This characteristic makes Sr-90 an ideal candidate for assessing the detector's capability to discern MIPs, a fundamental prerequisite for detecting a broader spectrum of particles.

Preliminary Steps: Pedestal and Calibration Runs

Prior to the full run analysis, preliminary steps were undertaken to ensure the accuracy and reliability of the experimental results. These steps, as explained before, pedestal and calibration runs, which are critical for establishing baseline measurements and calibrating the sensors, respectively.

Full Run Results

The full run results, encapsulated in Figure 3.7, exhibit the signal response of the Silicon Strip Detectors to Strontium-90 beta emissions, post the pedestal and common mode noise subtraction, as previously elucidated. The response is quantified in both Analog-to-Digital Converter (ADC) counts and the corresponding electron counts, with the conversion factor, approximately 300, derived from the gain per channel.

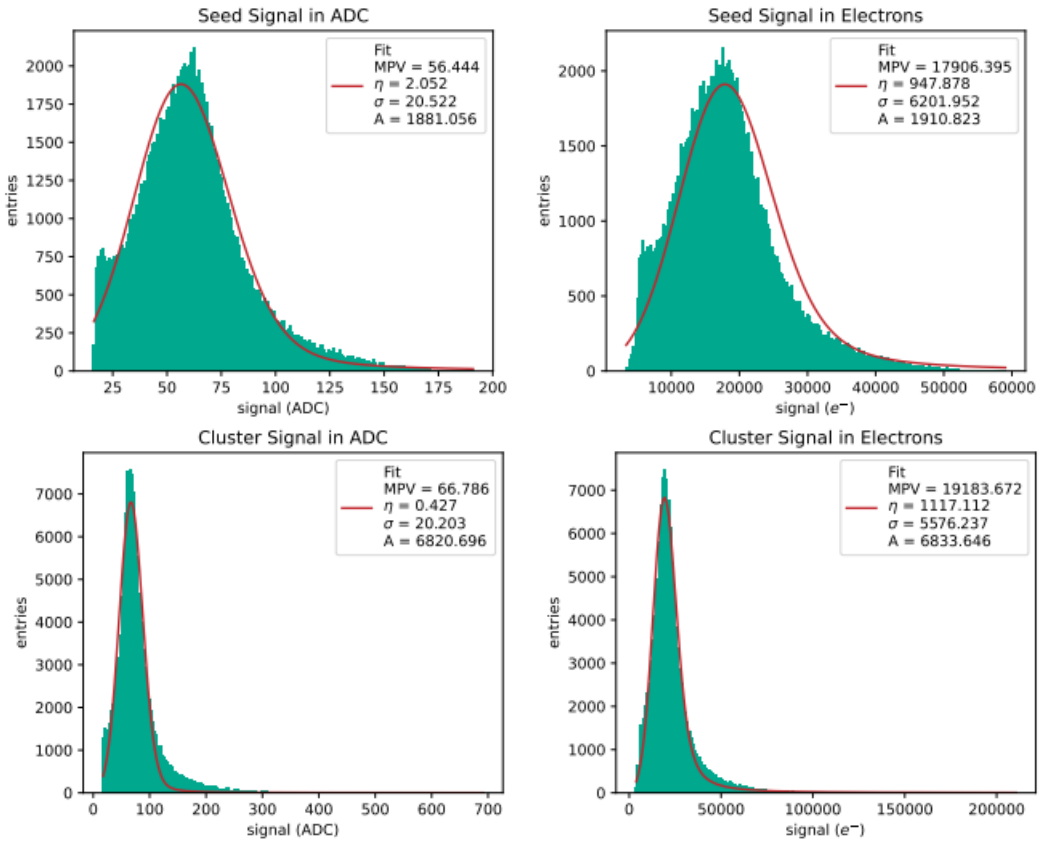

Figure 3.7: Full run results displaying the seed and cluster signal in ADC counts and electron counts.

Signal Distribution Analysis

The signal distributions for both the seed and cluster signals are modeled by Landau distributions, characteristic of the energy loss of charged particles (such as beta particles) traversing the detectors. The parameters obtained from the fits are indicative of the detector performance under exposure to a radioactive source.

1. Seed Signal

In ADC Counts

The seed signal in ADC counts reveals a Most Probable Value (MPV) of 56.444 ADC counts, with a standard deviation (σ) of 20.852. The distribution reflects the initial interaction of the beta particles with the detector, where the Landau peak corresponds to the MPV, and the observed spread (σ) is due to the inherent variations in the particle interactions and electronic noise.

In Electron Counts

When converted to electron counts, the seed signal exhibits an MPV of 17906.395 e^-, with a σ of 6910.952. This conversion elucidates the actual charge collected at the most probable energy deposition event, adjusted for the gain per channel.

2. Cluster Signal

In ADC Counts

The cluster signal in ADC counts is described by an MPV of 66.786, a σ of 20.203. This cluster signal encompasses the collective response from multiple strips, providing a more integrated representation of the interaction.

In Electron Counts

The cluster signal in electron counts, a more direct measure of the deposited energy, shows an MPV of 19183.672 e^-, a σ of 5536.237. The larger MPV compared to the seed signal indicates the summation effect of the cluster formation.

Implications of the Landau Distribution and Delta Electrons

The characteristic Landau distribution observed in both the seed and cluster signals is further extended by the presence of delta electrons, as evidenced by the pronounced long tails in the distributions. Delta electrons, or high-energy secondary electrons, are generated when the incident beta particles impart sufficient energy to dislodge electrons from atoms within the detector material. These secondary electrons can travel significant distances, depositing energy far from the initial interaction site, thus contributing to the long tail of the Landau distribution.

Noise Consideration and Signal Integrity

It is imperative to acknowledge that prior to the analysis, meticulous noise reduction steps were implemented. The pedestal run, which measures the output of the detector when no external signal is present, and the common mode noise subtraction, which corrects for variations in the detector's response due to environmental or electronic influences, were both critical for isolating genuine particle-induced signals from background noise. The successful application of these noise filtering techniques was confirmed by the signal clarity in the resultant distributions, thereby allowing for an accurate assessment of the detector's sensitivity and resolution in the context of MIP detection.

These preparatory steps, fundamental to the integrity of the data, permitted the subsequent analyses to focus on the physics of particle detection and interaction without the confounding influence of systematic noise. As a result, the reported signal characteristics are representative of true events, facilitating a robust interpretation of the detector's performance during the full run.

Bibliography

[1] Given Literature: Einführung in das kernphysikalische Praktikum, "Blue Book" with the descriptions of the experiments in the nuclear and particle physics section.

[2] EASY: Educational Alibava System, Technical Documentation, `https://inspirehep.net/files/24f32e93d201b37229d08262c336d5ee`